Separation Science and Technology
Publication details, including instructions for authors and subscription information:
http://www.informaworld.com/smpp/title~content=t713708471

Electrical Aspects of Adsorbing Colloid Flotation. XIII. Adsorption onto Surfaces with Positive and Negative Sites

J. Michael Brown[a]; David J. Wilson[a]
[a] DEPARTMENTS OF CHEMISTRY AND CHEMICAL ENGINEERING, VANDERBILT UNIVERSITY NASHVILLE, TENNESSEE

To cite this Article Brown, J. Michael and Wilson, David J.(1981) 'Electrical Aspects of Adsorbing Colloid Flotation. XIII. Adsorption onto Surfaces with Positive and Negative Sites', Separation Science and Technology, 16: 7, 773 — 792
To link to this Article: DOI: 10.1080/01496398108058127
URL: http://dx.doi.org/10.1080/01496398108058127

SEPARATION SCIENCE AND TECHNOLOGY, 16(7), pp. 773–792, 1981

Electrical Aspects of Adsorbing Colloid Flotation. XIII. Adsorption onto Surfaces with Positive and Negative Sites

J. MICHAEL BROWN and DAVID J. WILSON*

DEPARTMENTS OF CHEMISTRY AND CHEMICAL ENGINEERING
VANDERBILT UNIVERSITY
NASHVILLE, TENNESSEE 37235

Abstract

The adsorption of anions and cations, including amphipathic ions, onto flocs having both positive and negative adsorption sites was examined theoretically. The effects of ionic strength, substrate concentration, site lattice spacing, adsorption energy, and (in the case of amphipaths) hydrocarbon chain length were examined. An approximate thermodynamic approach was used.

INTRODUCTION

Theoretical studies of foam flotation techniques have involved the use of several adsorption models. Our group has developed a number of methods for calculating adsorption isotherms of surfactant ions adsorbing onto floc particles (*1–4*). The formation of a condensed phase (hemimicelle) on the floc surface is a cooperative phenomenon resulting from the van der Waals stabilization energy of the hydrocarbon tails of the surfactant ions. Fuerstenau et al. found that this condensed phase forms at lower surfactant concentrations as the length of the hydrocarbon chain increases (*5*, *6*). The adsorption isotherms depend strongly on ionic strength since nonamphipathic ions compete with the surfactant ions for adsorption sites on the charged solid surface. Wilson gave a treatment of this cooperative phenomenon (*7*) by means of an approximate method given by Fowler and Guggenheim (*8*). He estimated the binding energy of the surfactant ion with the surface by calculating the electric potential in the vicinity of the solid surface by means of a modified Poisson-Boltzmann equation. The results showed very

*To whom correspondence should be addressed.

reasonable dependence of the adsorption isotherms on surface potential, van der Waals interaction energy, temperature, and ionic strength. The effect of varying surfactant chain length was also demonstrated and showed the expected results. In a later paper Currin et al. investigated the effect of surfactant displacement by foreign ions. They gave a statistical mechanical analysis of this phenomenon which they verified experimentally (*2*). Clarke et al. presented a theoretical analysis of the effects of specifically adsorbed ions on floc surface potentials and gave some experimental results of these effects on floc foam flotation (*9*).

At higher surfactant concentrations it is possible for another type of cooperative phenomenon to occur; the formation of a second condensed layer of surfactant on top of the hemimicelle on the solid surface. This makes the surface hydrophilic and prevents the bubble attachment that is necessary for flotation. Wilson and Kennedy used statistical mechanics to model this phenomenon and also gave experimental verification of their model (*3*). Kiefer has refined and improved the model of surfactant adsorption, taking into account the effects of coulombic repulsion between the ionic heads in addition to the van der Waals' attraction between the hydrocarbon tails of the adsorbed surfactant ions (*4*).

Here we describe a more complex situation. We generalize our system to include both cations and anions absorbed onto a solid surface that contains both positive and negative sites. The theory used to model this system is extended to include the adsorption of a cationic and an anionic surfactant onto this type of surface. A model which assumes two sets of discrete adsorption sites was first used by Gaudin and Fuerstenau in connection with ore flotation (*10*).

ANALYSIS

We choose as our model system the adsorption of hydronium ions. H_3O^+, and hydroxyl ions, OH^-, onto a surface which consists of an equal number of positive sites A and negative sites B, each arranged in a square grid as shown in Fig. 1. At high pH the A sites adsorb OH^- to become electrically neutral, and at low pH the B sites are neutralized by adsorption of H_3O^+ ions. We consider only Langmuir-type adsorption; i.e., each site has either a $+1$ or -1 charge and can adsorb only one ion. We let l equal the distance between the centers of each type of site; a, the distance of closest approach of an OH^- ion to an A site; and b, the distance of closest approach of an H_3O^+ ion to a B site. For each A site we consider electrical interactions only from the four neighboring B sites, and for each B site we take into account interactions only from the four neighboring A sites. Thus interactions over distances greater than l are ignored. The screening of more long-range coulombic interactions

by ionic atmospheres makes this a reasonable assumption. To calculate the electric potential in the vicinity of a site we use a form of the Poisson-Boltzmann equation that takes into account the finite volumes of the ions comprising the ionic atmosphere and utilizes our assumption that the charge density on the planar surface is contained in discrete, evenly spaced hemispherical sites (*11*). The equation is

$$\frac{1}{r^2}\frac{\partial}{\partial r}\left(r^2\frac{\partial \psi}{\partial r}\right) = \frac{\mathrm{A}\sinh\beta'\psi}{1 + \mathrm{B}\cosh\beta'\psi} \tag{1}$$

where $\psi(r)$ = electric potential at a distance r from the center of the charged site

$$\mathrm{A} = \frac{8\pi z e c_\infty}{(1 - 2c_\infty/c_{\max})D}$$

$$\mathrm{B} = \frac{2c_\infty}{(c_{\max} - 2c_\infty)}$$

$$\beta' = ze/kT$$

D = dielectric constant of water

ze = | charge| of 1–1 inert electrolyte ions

c_∞ = concentration in bulk solution of 1–1 electrolyte establishing the ionic atmosphere

$c_{\max}$ = maximum possible concentration of the electrolyte

All quantities are in cgs units per ion. Equation (1) is solved numerically by finite difference approximations of the derivatives using

$$\psi_{n-1} = \psi_n\frac{2r_n}{r_{n-1}} - \psi_{n+1}\frac{r_{n+1}}{r_{n-1}} + \frac{r_n}{r_{n-1}}\Delta r^2\frac{\mathrm{A}\sinh\beta'\psi_n}{1 + \mathrm{B}\cosh\beta'\psi_n} \tag{2}$$

and changing the boundary equations

$$\psi(\infty) = 0 \tag{3}$$

and

$$\frac{\partial\psi}{dr}(x) = \frac{-2Q}{x^2D} \tag{4}$$

to

$$\psi(r_N) = 0 \tag{5}$$

and

$$\frac{\psi_2 - \psi_1}{\Delta r} = \frac{-2Q}{x^2 D} \tag{6}$$

where $x = a$ or b

$r_N = 4$ Debye lengths

$\psi_n = \psi(r_n)$

$Q =$ charge of central site ($\pm e$ for vacant site, 0 for occupied site)

We calculate the values of $\psi(r)$ as follows: At a distance equal to approximately 4 Debye lengths we set $\psi(r_N) = 0$ and $\psi(r_{N-1}) = 1.0 \times 10^{-8}$; then from Eq. (2) the remaining ψ's to $\psi(r_1)$ are calculated. From this set of ψ's we calculate

$$\text{ratio} = \frac{2Q\Delta r}{x^2 D[\psi(r_2) - \psi(r_1)]}$$

to determine if the second boundary condition specified by Eq. (6) is satisfied. If not, we set new $\psi(r_{N-1}) =$ old $\psi(r_{N-1}) \cdot$ ratio, and start over until the set of ψ's satisfies both boundary equations. This same analysis has been successfully applied to calculating adsorption isotherms of ionic surfactants on a charged surface by Kiefer and Wilson (*4*).

The electric potential for an uncharged site (an occupied site) is zero, and for a site with charge ± 1, the electric potential at distance r from the site is $\pm\psi(r)$. We write the increase in energy when a H_3O^+ ion is adsorbed on a B site as (approximately)

$$\chi_{H_3O^+} = [\psi(b) + 4(1 - \theta_{OH^-})\psi(l)]_e + \Delta\mu^\circ_{H_3O^+} \tag{7}$$

where θ_{OH^-} = the fraction of A sites occupied by OH^- ions

$\Delta\mu^\circ_{H_3O^+}$ = the difference in standard state chemical potentials between an H_3O^+ ion in solution and an H_3O^+ ion adsorbed on a B site

Similarly, we can write the increase in energy when an OH^- ion is adsorbed on an A site as

$$\chi_{OH^-} = -[\psi(a) + \psi(1 - \theta_{H_3O^+})\psi(l)]e - \Delta\mu^\circ_{OH^-} \tag{8}$$

where $\theta_{H_3O^+} =$ the fraction of B sites occupied by H_3O^+ ions

$\Delta\mu^{\circ}_{OH^-}$ = the difference in standard state chemical potentials between an OH^- ion in solution and an OH^- ion adsorbed on an A site

It should be noted that this model underestimates the cooperative interaction between the two sets of sites. We are assuming a random distribution of adsorption, not taking into account the stabilization afforded by occupied neighboring sites. The approach we are using gives a first-order perturbation estimate of the interaction. An exact solution appears to be extremely difficult and complex. Now we write the chemical potential of an adsorbed H_3O^+ ion as

$$\mu^{(a)}_{H_3O^+} = \mu^{\circ(a)}_{H_3O^+} + kT\log_e \frac{\theta_{H_3O^+}}{1-\theta_{H_3O^+}} - [|\psi(b)| - 4(1-\theta_{OH^-})|\psi(l)|]e \tag{9}$$

and the chemical potential of an adsorbed OH^- ion is

$$\mu^{(a)}_{OH^-} = \mu^{\circ(a)}_{OH^-} + kT\log_e \frac{\theta_{OH^-}}{1-\theta_{OH^-}} - [|\psi(b)| - 4(1-\theta_{H_3O^+})|\psi(l)|]e \tag{10}$$

For the ions in solution the chemical potential is given as

$$\mu^{(s)}_{H_3O^+} = \mu^{\circ(s)}_{H_3O^+} + kT\log_e(\gamma_{H_3O^+}c_{H_3O^+}) \tag{11}$$

where $\gamma_{H_3O^+}$ = activity coefficient of H_3O^+ ion in solution

$c_{H_3O^+}$ = concentration of H_3O^+ ion in solution

and

$$\mu^{(s)}_{OH^-} = \mu^{\circ(s)}_{OH^-} + kT\log_e(\gamma_{OH^-}c_{OH^-}) \tag{12}$$

where γ and c_{OH^-} pertain to OH^- ions in solution. At equilibrium we can write

$$\mu^{(a)}_{H_3O^+} = \mu^{(s)}_{H_3O^+} \tag{13}$$

and

$$\mu^{(a)}_{OH^-} = \mu^{(s)}_{OH^-} \tag{14}$$

Combining Eqs. (9), (11), and (13) gives

$$\mu^{\circ(s)}_{H_3O^+} + kT\log_e(\gamma_{H_3O^+}c_{H_3O^+}) = \mu^{\circ(a)}_{H_3O^+} + kT\log\frac{\theta_{H_3O^+}}{1-\theta_{H_3O^+}} - [|\psi(b)| - 4(1-\theta_{OH^-})|\psi(l)|]e \tag{15}$$

and combining Eqs. (10), (12), and (14) gives

$$\mu^{\circ(s)}_{OH^-} + kT\log_e(\gamma_{OH^-}c_{OH^-}) = \mu^{\circ(a)}_{OH^-} + kT\log_e \frac{\theta_{OH^-}}{1-\theta_{OH^-}} - [\,|\,\psi(a)\,| - 4(1-\theta_{H_3O^+})\,|\,\psi(l)\,|\,]e \quad (16)$$

Rearranging (15) and (16) gives

$$\theta_{H_3O^+} = \frac{\exp(\mathrm{ARG}_{H_3O^+})}{1+\exp(\mathrm{ARG}_{H_3O^+})} \quad (17)$$

where

$$\mathrm{ARG}_{H_3O^+} = \frac{\Delta\mu^{\circ}_{H_3O^+}}{kT} + \log_e(\gamma_{H_3O^+}c_{H_3O^+}) + [\,|\,\psi(b)\,| - 4(1-\theta_{OH^-})\,|\,\psi(l)\,|\,]e/kT$$

and

$$\theta_{OH^-} = \frac{\exp(\mathrm{ARG}_{OH^-})}{1+\exp(\mathrm{ARG}_{OH^-})} \quad (18)$$

where

$$\mathrm{ARG}_{OH^-} = \frac{\Delta\mu^{\circ}_{OH^-}}{kT} + \log_e(\gamma_{OH^-}c_{OH^-}) + [\,|\,\psi(a)\,| - 4(1-\theta_{H_3O^+})\,|\,\psi(l)\,|\,]e/kT$$

We now have two coupled equations for $\theta_{H_3O^+}$ and θ_{OH^-}. These can be solved iteratively by taking as a first approximation the equations resulting from neglecting all interactions between the two sets of sites; this is

$$\theta_{OH^-\,\mathrm{starter}} = \frac{\gamma_{OH^-}c_{OH^-}\exp(\mathrm{ARG})}{1+\gamma_{OH^-}c_{OH^-}\exp(\mathrm{ARG}_s)} \quad (19)$$

where

$$\mathrm{ARG}_s = \frac{\Delta\mu^{\circ}_{OH^-} + e\,|\,\psi(a)\,|}{kT}$$

In the enclosed area shown in Fig. 1 we see that for an area of $\frac{9}{2}l^2$ there are 2.25 A sites and 2.25 B sites. The mean surface charge density, $\bar{\sigma}$, is written as

$$\bar{\sigma} = \frac{2.25}{\frac{9}{2}l^2}[(1 - \theta_{OH^-}) - (1 - \theta_{H_3O^+})]e$$

$$= \frac{e}{2l^2}(\theta_{H_3O^+} - \theta_{OH^-}) \tag{20}$$

Another form of the Poisson-Boltzmann equation given in Eq. (1) that is valid for one-dimensional planar problems is

$$\frac{d^2\psi}{dx^2} = \frac{\text{A sinh } (ze\psi/kT)}{1 + \text{B cosh } (ze\psi/kT)} \tag{21}$$

where A and B have the same meaning as before. A first integral to this equation which satisfies the boundary condition

$$\frac{d\psi}{dx} \to 0 \text{ as } x \to \infty$$

is

$$\frac{d\psi}{dx} = \frac{-\psi_0}{|\psi_0|}\left[\frac{2AkT}{ze\text{B}} \log_e\left(\frac{1 + \text{B cosh } (ze\psi/kT)}{1 + \text{B}}\right)\right]^{1/2} \tag{22}$$

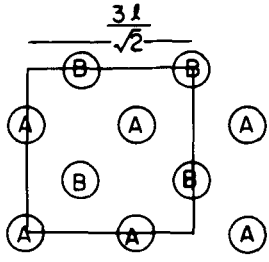

FIG. 1. Diagram of the model of the solid surface on which adsorption takes place. A sites are positively charged, B sites are negative.

where ψ_0 is the mean surface potential. The electrical neutrality requirement permits us to write

$$\bar{\sigma} = \frac{-D}{4\pi} \frac{d\psi(0)}{dx} \tag{23}$$

Substituting Eq. (22) into Eq. (23) and solving for ψ_0 gives

$$\psi_0 = \frac{\bar{\sigma} kT}{|\bar{\sigma}| ze} |\cosh^{-1}(\mathrm{ARG})| \tag{24}$$

where

$$\mathrm{ARG} = \frac{(1 + \mathrm{B}) \exp\left[\left(\frac{4\pi\bar{\sigma}}{D}\right)^2 \frac{ze\mathrm{B}}{2\mathrm{A}kT}\right] - 1}{\mathrm{B}}$$

and $\bar{\sigma}$ is given by Eq. (20). We can now calculate ψ_0 from θ_{OH^-} and $\theta_{H_3O^+}$ and examine plots of mean surface potential, ψ_0 versus pH.

RESULTS

In Fig. 2 the effect of changing l, the distance between like sites, on the absorption isotherms is demonstrated. Because varying l only changes the

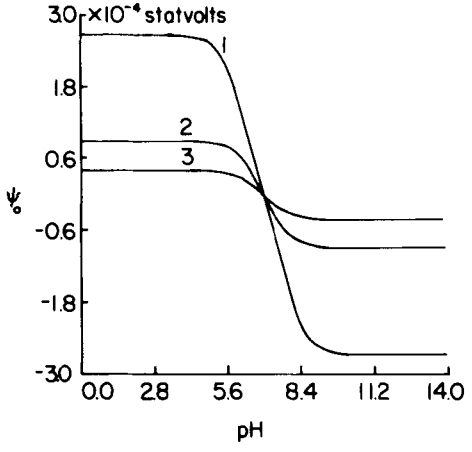

FIG. 2. Effect of l, the distance between sites, on the dependence of ψ_0 on pH. l = 10 Å (1), 20 Å (2), 30 Å (3).

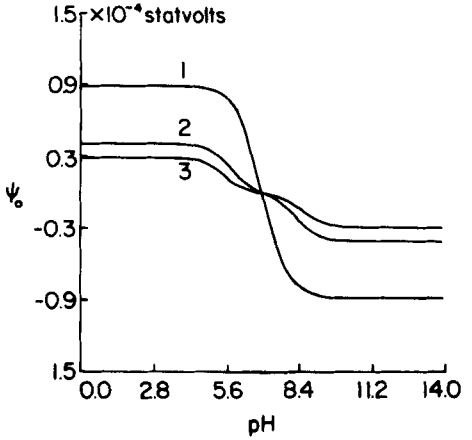

FIG. 3. Effect of ionic strength on the dependence of ψ_0 on pH. $c_\infty = 0.1\ M$ (1), $0.5\ M$ (2), $1.0\ M$ (3).

surface charge density, the pH of the zero surface potential is unchanged. However, decreasing l increases the magnitude of ψ_0 in each limiting pH range because of the increase in surface charge density.

Figure 3 shows the effect of changing the inert electrolyte concentration on the adsorption isotherms. As the ionic strength increases, the electric potential of a charged site is more effectively screened by the ions in the

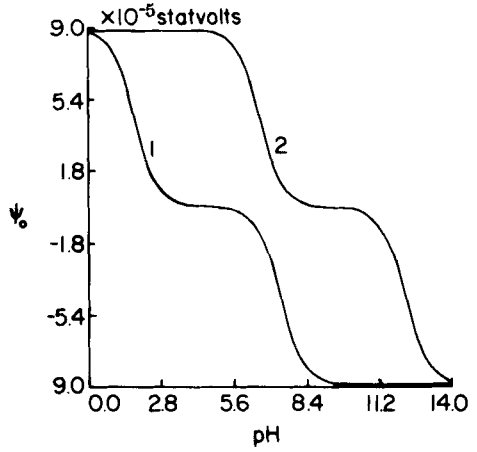

FIG. 4. Effect of binding energy on the dependence of ψ_0 on pH. $\Delta\mu^\circ_{OH^-} \neq \Delta\mu^\circ_{H_3O^+}$ $\Delta\mu^\circ_{H_3O^+} = -2.0 \times 10^{-12}$, $\Delta\mu^\circ_{OH^-} = -1.54 \times 10^{-12}$ (1); $\Delta\mu^\circ_{H_3O^+} = 1.54 \times 10^{-12}$, $\Delta\mu^\circ_{OH^-} = -2.0 \times 10^{-12}$ ergs (2).

electric double layer. We see in Fig. 3 that increasing ionic strength decreases the slope of the isotherms and decreases the limiting values of ψ_0 due to the screening effect.

Figure 4 shows the dependence of the adsorption isotherms on the relative binding energies of the H_3O^- and OH^- ions. Decreasing $\Delta\mu^\circ_{OH^-}$ moves the point of zero charge (p.z.c.) to a higher pH because the OH^- ions are adsorbed less readily. Similarly decreasing $\Delta\mu^\circ_{H_3O^+}$ moves the p.z.c. to lower pH values since H_3O^- ions are not as easily adsorbed. Decreasing both $\Delta\mu^\circ_{H_3O^+}$ and $\Delta\mu^\circ_{OH^-}$ causes the p.z.c. to exist over an increasingly broad range of pH values as shown in Fig. 5. This is because OH^- ions are not adsorbed appreciably until higher pH values and H_3O^+ ions are not adsorbed strongly until lower pH values. We note that the binding energies used to calculate the adsorption isotherms are negative because of the large coulombic interactions between the ions and their respective adsorption sites.

Figures 6 and 7 show the effect of varying the assumed radii of the H_3O^+ and OH^- ions. Changing r_{OH^-} and $r_{H_3O^+}$ by the same amount does not affect the p.z.c. However, the larger $r_{H_3O^+}$, the larger the distance of closest approach of an H_3O^+ ion to a B site. The electric potential is smaller at greater distances; therefore the coulombic attraction is diminished. This results in a lower pH to give the same amount of adsorption as before when the radius was smaller. This same argument applies to changing the radius of an OH^- ion; and changing r_{OH^-} and $r_{H_3O^+}$ by different amounts will change the pH value of the p.z.c. for this same reason.

Figures 8 and 9 are plots of $\theta_{H_3O^+}$ and θ_{OH^-} vs pH, respectively. Because

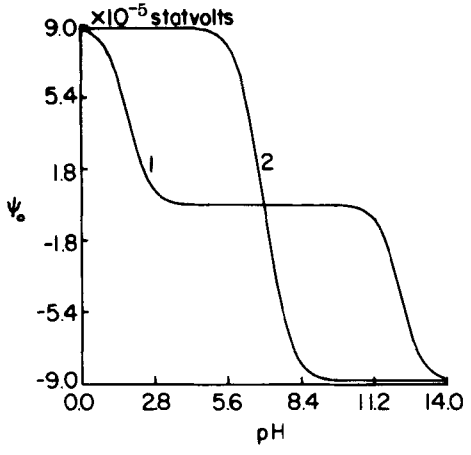

FIG. 5. Effect of binding energy on the dependence of ψ_0 on pH, $\Delta\mu^\circ_{OH^-} = \Delta\mu^\circ_{H_3O^+}$. $\Delta\mu^\circ = -2.0 \times 10^{-12}$ (1), $= -1.54 \times 10^{-12}$ (2) ergs.

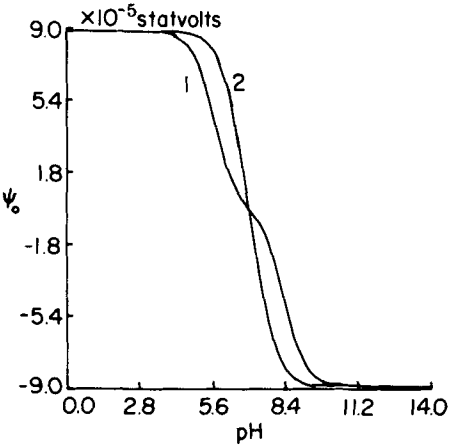

FIG. 6. Effect of the assumed radii for H_3O^+ and OH^- on the dependence of ψ_0 on pH, $r_{H_3O^+} = r_{OH^-}$. r = 2 Å (1), r = 1 Å (2).

the parameters for the H_3O^+ ions and the OH^- ions are assumed to be the same, the curves are symmetric with respect to each other about the p.z.c., which was designed to occur at a pH of 7.0. We can now choose our values of $\Delta\mu^\circ_{H_3O^+}$, $\Delta\mu^\circ_{OH^-}$, and l's to represent an actual surface. Zeta potential measurements can give us the p.z.c. which in turn can be used to calculate the parameters just mentioned. The qualitative correctness of the results suggests that we can use this theory in prediciting the performance of particulate foam

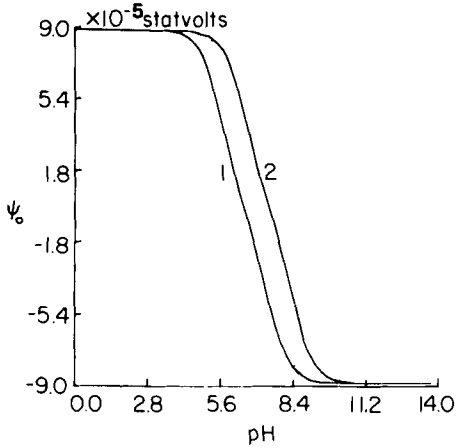

FIG. 7. Effect of the assumed radii for H_3O^+ and OH^- on the dependence of ψ_0 on pH, $r_{H_3O^+} \neq r_{OH^-}$. $r_{H_3O^+} = 2$ Å, $r_{OH^-} = 1$ Å (1); $r_{H_3O^+} = 1$ Å, $r_{OH^-} = 2$ Å (2).

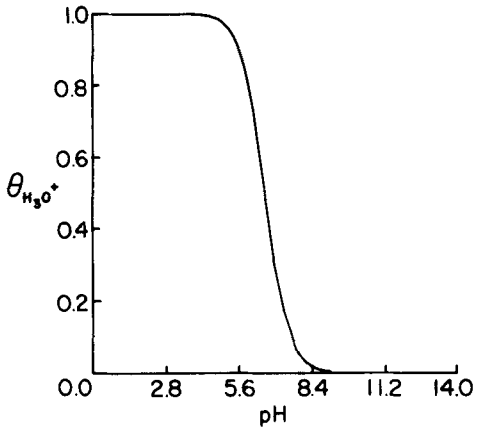

FIG. 8. Dependence of $\theta_{H_3O^+}$, the fraction of negative sites occupied, on pH.

flotation techniques in the removal of environmental pollutants from waste waters, the concentration of valuable metals from ore leachate solutions, and the beneficiation of ores by froth flotation.

EXTENSION TO SURFACTANT IONS

We now consider the application of the previously described model to the adsorption of a cationic and an anionic surfactant together in solution onto the previously described surface. We assume here that the interaction of the hydrocarbon tails is sufficiently weak that condensation does not occur. The

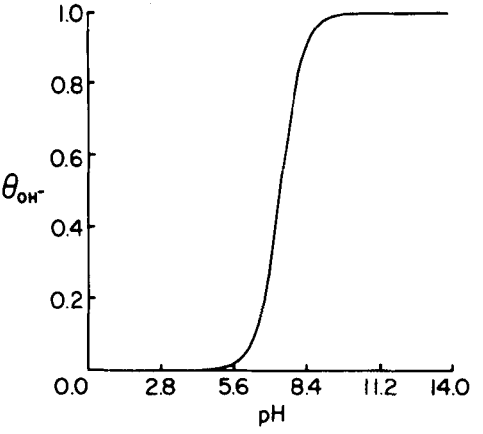

FIG. 9. Dependence of θ_{OH^-}, the fraction of positive sites occupied, on pH.

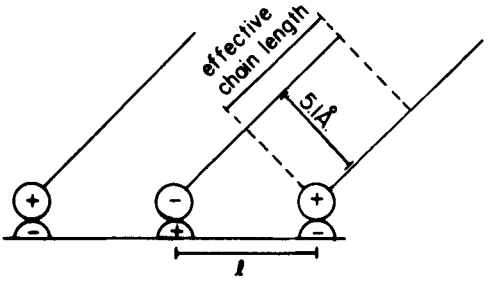

FIG. 10. Configuration of the adsorbed surfactant ions.

charges of the surfactants are +1 and −1; therefore no coulombic repulsion or attraction between adsorbed ion sites exists. The increase in energy when a cationic surfactant molecule, s^+, is adsorbed on a negative B site is

$$\chi_+ = [-|\psi(b)| + 4(1 - \theta_{s^-})|\psi(l)|]e - 4nc_2\theta_- + \Delta\mu_{s^+}^\circ \qquad (25)$$

where n = effective number of CH_2 and CH_3 groups in the cationic surfactant and anionic surfactant chains

c_2 = cooperative van der Waal's stabilizing energy per CH_2 group. This was estimated to be 2.08×10^{-14} erg (see Ref. *4*)

θ_{s^+}, θ_{s^-}, and $\Delta\mu_{s^-}^\circ$ are the same as previously described.

For the anionic surfactant, s^-, adsorbed onto a positive A site the increase in energy is

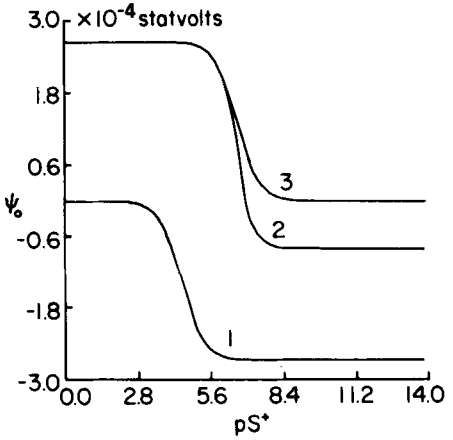

FIG. 11. Effect of anionic surfactant concentration on the dependence of ψ on pS^+. $pS^- =$ 0 (1), = 7.0 (2), = 10.0 (3).

$$\chi_- = [-|\psi(a)| + 4(1 - \theta_{s+})|\psi(l)|]e - 4nc_2\theta_{s+} + \Delta\mu_s^\circ - \quad (26)$$

where $\Delta\mu_x^\circ$- has its usual meaning. The chemical potentials of the two adsorbed surfactant species are then

$$\mu_{s+}^{(a)} = \mu_+^{\circ(a)} + kT \log_e \frac{\theta_{s+}}{1 - \theta_{s+}} - [|\psi(b)| - 4(1 - \theta_{s-})|\psi(l)|]e$$

$$- 4nc_2\theta_{s-} + \Delta\mu_{s+}{}^\circ \quad (27)$$

and

$$\mu_{s-}{}^{(a)} = \mu_{s-}^{\circ(a)} + kT \log_e \frac{\theta_{s-}}{1 - \theta_{s-}}[|\psi(a)| - 4(1 - \theta_{s+})|\psi(l)|]e$$

$$- 4nc_2\theta_{s+} + \Delta\mu_{s-}{}^\circ \quad (28)$$

The effective diameter of the hydrocarbon chain is approximately 5.1 Å. The distance between carbon atoms in the chain is approximately 1.43 Å. From Fig. 10 we can calculate an effective chain length taking into account the nonvertical orientations of the surfactant ions. The effective chain length, EFC, is

$$\mathrm{EFC} = n1.43 - \frac{5.1}{\sin\left[\arctan\left(\frac{5.1}{l}\right)\right]} \quad (29)$$

where n = average number of CH_2 and CH_3 groups in the two surfactant species. Then n', the effective number of CH_2 and CH_3 groups, is given by

$$n' = \mathrm{EFC}/1.43 \quad (30)$$

(Note: To be as accurate as possible in simulating the actual orientations of the surfactant ions adsorbed on the solid surface, n' is not necessarily an integer value.)

As before, the chemical potentials of the ions in solution are written as

$$\mu_{s-}{}^{(s)} = \mu_{s+}^{\circ(s)} + kT \log_e (\gamma_{s-}c_{s-}) \quad (31)$$

and

$$\mu_{s-}{}^{(s)} = \mu_{s-}^{\circ(s)} + kT \log_e (\gamma_{s-}c_{s-}) \quad (32)$$

At equilibrium the chemical potentials of the ions in solution and adsorbed can be equated, giving the following expressions for θ_{s+} and θ_{s-}:

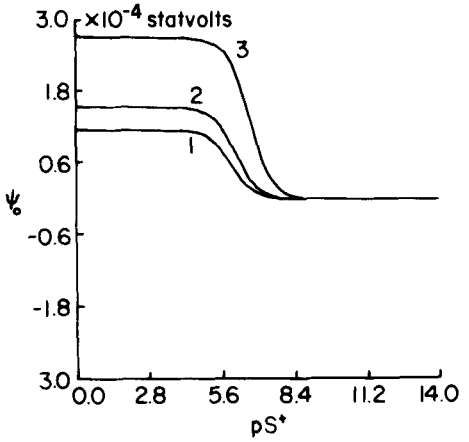

FIG. 12. Effect of ionic strength on the dependence of ψ_0 on pS^+ for $pS^- = 14$. $c_\infty = 1.0\ M$ (1), $= 0.5\ M$ (2), $= 0.1\ M$ (3).

$$\theta_{s^+} = \frac{\exp(ARG_{s^+})}{1 + \exp(ARG_{s^+})} \tag{33}$$

and

$$\theta_{s^-} = \frac{\exp(ARG_{s^-})}{1 + \exp(ARG_{s^-})} \tag{34}$$

where

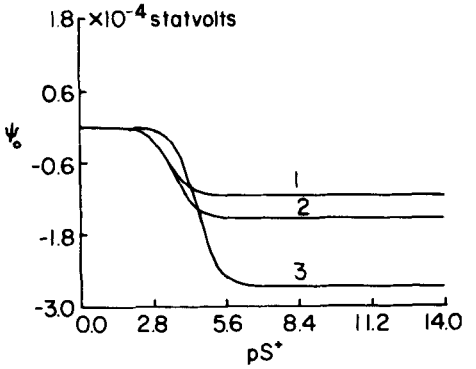

FIG. 13. Effect of ionic strength on the dependence of ψ_0 on pS^+ for $pS^- = 0.0$. c_∞ 0.1 M (1), $= 0.5\ M$ (2), $= 1.0\ M$ (3).

$$\mathrm{ARG}_{s+} = \frac{\Delta\mu_{s+}^{\circ}}{kT} + \log_e(\gamma_{s+}c_{s+}) + [\,|\,\psi(b)\,|$$

$$+ 4(1 - \theta_{s-})\,|\,\psi(l)\,|\,]\,\frac{e}{kT} + \frac{4nc_2\theta_{s-}}{kT}$$

and

$$\mathrm{ARG}_{s-} = \frac{\Delta\mu_{s-}^{\circ}}{kT} + \log_e(\gamma_{s-}c_{s-}) + [\,|\,\psi(a)\,|$$

$$+ 4(1 - \theta_{s+})\,|\,\psi(l)\,|\,]\,\frac{e}{kT} + \frac{4nc_2\theta_{s+}}{kT}$$

The mean surface charge density and mean surface potential can be calculated from the values for θ_{s+} and θ_{s-} as before.

RESULTS FOR SURFACTANTS

Figure 11 is plot of mean surface potential, ψ_0, vs the negative logarithm of the cationic surfactant concentration, pS^+, for three different values of pS^-, the negative logarithm of the anionic surfactant concentration. In each case the value of ψ_0 decreases with decreasing cationic surfactant concentration (increasing pS^+) because a larger number of negative adsorption sites are left unoccupied. As more positive sites are filled, the decrease in ψ_0 is enhanced, as shown by the isotherms for increasing anionic surfactant concentration (decreasing pS^-).

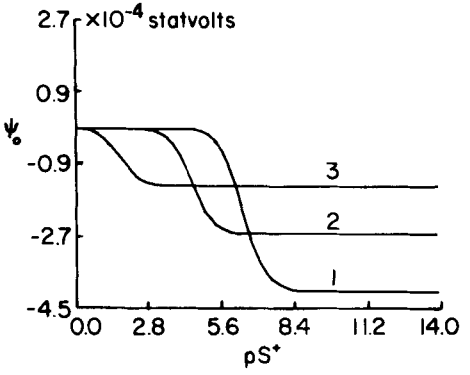

FIG. 14. Effect of l, the distance between the sites, on the dependence of ψ_0 on pS^+ for $pS^- = 0.0$. $l = 7$ Å (1), $= 10$ Å (2), $= 15$ Å (3).

In Figs. 12 and 13 we examine the effect of ionic strength on the adsorption isotherms for two different values of $[S^-]$, 1×10^{-14} and 1.0 M, respectively. Each figure shows that as the ionic strength is increased the sites are more effectively screened and ψ_0 is decreased for constant values of cationic surfactant concentration.

Figures 14 and 15 demonstrate the effect of varying the distance between adsorption sites, l, for $pS^- = 0$ and $pS^- = 14$, respectively. Increasing l always decreases the magnitude of the surface charge density. In Fig. 14, where the concentration of S^- is large, the unoccupied sites that contribute to the charge density are negative and we see that increasing l causes ψ_0 to assume smaller negative values. For a small S^- concentration, as in Fig. 15, the occupied sites are positive and ψ_0 decreases with increasing l. Figure 15 also shows that in the case of small concentrations of both S^- and S^+, the number of unoccupied positive and negative sites are nearly equal and cancel out to give a value of zero for ψ_0 which is not dependent on l.

Figure 16 shows the dependence of the isotherms on the relative binding energies of the two surfactant species. As the binding energy of the cationic surfactant is increased, the surface adsorption, indicated by an abrupt increase in the slope of the isotherm, is shifted to lower S^+ concentrations, as would be expected. As the binding energy of S^- is increased for a constant value of the binding energy of S^+, the positive sites become occupied to a greater extent, and the surface potential decreases due to the increase in negative charge. We note that, as mentioned in the previous analysis for the adsorption of hydroxyl and hydronium ions, that because the electric

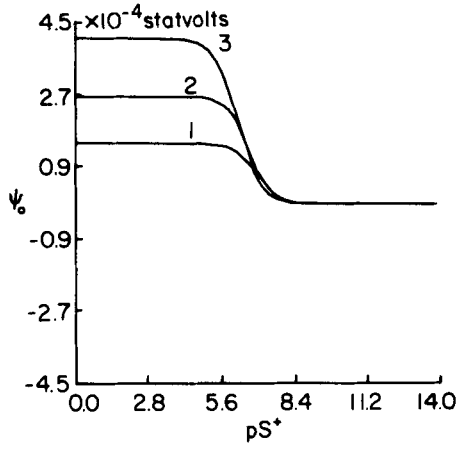

FIG. 15. Effect of l, the distance between the sites, on the dependence of ψ_0 on pS^+ for $pS^- = 14$. $l = 15$ Å (1), $= 10$ Å (2), $= 7$ Å (3).

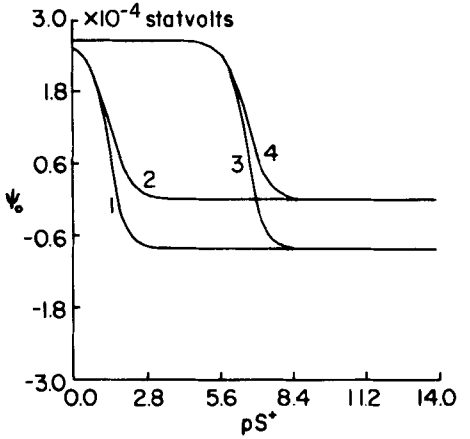

FIG. 16. Effect of the relative binding energies of the surfactant species on the dependence of ψ_0 on pS^+ for $pS^- = 7.0$. $\Delta\mu_s^{\circ -} = -2.0 \times 10^{-12}$, $\Delta\mu_s^{\circ +} = -1.5 \times 10^{-12}$ (1), $\Delta\mu_s^{\circ +} = \Delta\mu_s^{\circ -} = -2.0 \times 10^{-12}$ (2), $\Delta\mu_s^{\circ +} = \Delta\mu_s^{\circ -} = -1.5 \times 10^{-12}$ (3). $\Delta\mu_s^{\circ -} = -1.5 \times 10^{-12}$, $\Delta\mu_s^{\circ -} = -2.0 \times 10^{-12}$ (4) ergs.

interactions are large, the binding energies used to calculate the adsorption isotherms are negative. This may well be the case, since the entropies of the ions are lower in the adsorbed state.

Figure 17 shows the effect of varying the van der Waals stabilization energy between the hydrocarbon tails of adsorbed surfactant ions for a S^-

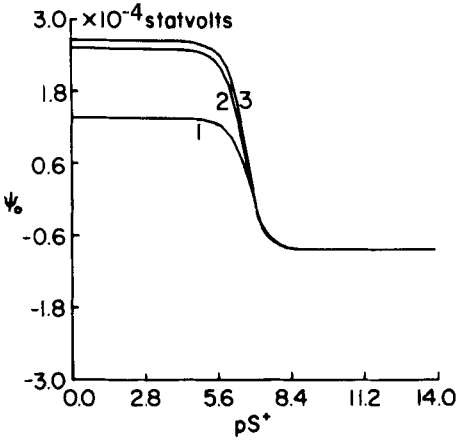

FIG. 17. Effect of the van der Waals stabilization energy on the dependence of ψ_0 on pS^+ for $pS^- = 7.0$. $c_2 = 0.0$ (1), $= 1.0 \times 10^{-14}$ (2), $= 2.08 \times 10^{-14}$ (3) ergs.

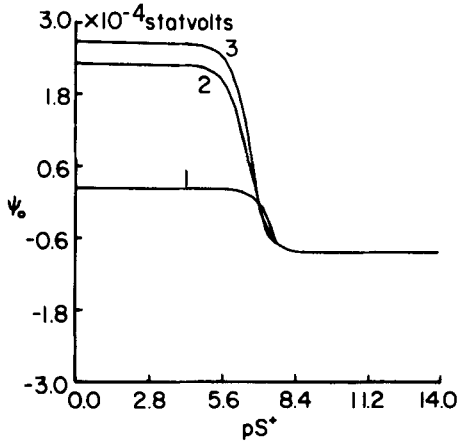

FIG. 18. Effect of hydrocarbon tail chain length on the dependence of ψ_0 on pS^+ for $pS^- = 7.0$. $n = 9$ (1), $= 7$ (2), $= 5$ (3).

concentration of 1×10^{-7} M. As the interaction energy is decreased, the extent of adsorption of S^+ ions decreases, and this increase in the number of unoccupied negative sites decreases ψ_0. Changing the number of CH_2 groups in the hydrocarbon tails also changes the interaction energy. Figure 18 shows the same effect just described. As the number of CH_2 groups increases, the adsorption of S^+ ions increases and the number of unoccupied negative sites increases. This increase in negative charge density decreases ψ_0.

CONCLUSIONS

The results of this model for the mixed adsorption of a cationic and anionic surfactant are in correct qualitative agreement with our intuitive expectations. We now have a theoretical basis for predicting the performance of particulate foam flotation in situations where the collector consists of mixed ionic species. Zeta potentials which can be obtained from electrophoretic mobility measurements can be used to calculate the mean surface electric potential. The theoretical treatment presented here could then be matched to the experimental data by changing quantities that were estimated in this initial study such as relative binding energies, ionic radii, and distance between sites. An understanding of the principles which govern the operation of foam flotation techniques is invaluable in applying these separation methods to the removal of environmental pollutants.

REFERENCES

1. D. J. Wilson, *Sep. Sci.*, *12*, 231 (1977).
2. B. L. Currin, F. J. Potter, D. J. Wilson, and R. H. French, *Sep. Sci. Technol.*, *13*, 285 (1978).
3. D. J. Wilson and R. M. Kennedy, *Ibid.*, *14*, 319 (1979).
4. J. E. Kiefer and D. J. Wilson, *Ibid.*, *15*, 57 (1980).
5. D. W. Fuerstenau, T. W. Healy, and P. Somasundaran, *Trans. AIME*, *229*, 321 (1964).
6. T. Wakamatsu and D. W. Fuerstenau, *Adv. Chem. Ser.*, *79*, 161 (1978).
7. D. J. Wilson, *Sep. Sci.*, *12*, 447 (1977).
8. R. Fowler and E. A. Guggenheim, *Statistical Thermodynamics*, Cambridge University Press, 1952, pp. 429–443.
9. A. N. Clarke, D. J. Wilson, and J. H. Clarke, *Sep. Sci. Technol.*, *13*, 573 (1978).
10. A. M. Gaudin and D. W. Fuerstenau, *Trans. AIME*, *202*, 958 (1955).
11. D. J. Wilson, *Sep. Sci.*, *11*, 391 (1976).

Received by editor January 19, 1981